Thermal fluctuations of the shapes of droplets in dense and compressed emulsions

Hu Gang,[1] A. H. Krall,[1,2] and D. A. Weitz[1]
[1]*Exxon Research and Engineering Company, Route 22E, Annandale, New Jersey 08801*
[2]*Physics Department, Princeton University, Princeton, New Jersey 08544*
(Received 23 June 1995)

We generalize the theory of diffusing-wave spectroscopy (DWS) to include the effects of fluctuations of the amplitudes of the scattered fields. Thus DWS can be used to probe the internal dynamics of flexible particles. We study the thermally induced shape fluctuations of monodisperse emulsion droplets as a function of the droplet volume fraction ϕ. We find that a droplet's mean-squared deviation from spherical shape increases with ϕ, while the characteristic rate of relaxation of the shape deformations decreases with ϕ. Our generalization of the theory of DWS allows us to measure the autocorrelation function of the fluctuating amplitude of the field scattered from a droplet. We use fluid dynamics and scattering theory to calculate this autocorrelation function theoretically for an isolated droplet. The significant contribution of many independent modes of deformation results in a distinctly nonexponential relaxation. The measured behavior agrees with the theory as ϕ approaches zero. At higher values of ϕ throughout the range of colloidal liquids we find a surprising scaling behavior, which implies that particle interactions bring about the enhancement and slowing down of shape fluctuations without altering the spectrum of excited deformation modes. We relate the form of the scaling function to the particle radial distribution function. In "compressed" emulsions with ϕ as high as 0.8, shape fluctuations may be the only dynamical behavior that can occur. We suggest that in these systems the amplitude of the shape fluctuations is related to the emulsion's elastic modulus.

PACS number(s): 68.10.−m, 82.70.Kj, 05.40.+j, 47.55.Dz

I. INTRODUCTION

Dispersions of one liquid in another immiscible liquid are called emulsions. Emulsions have long been of great practical interest; typical uses include foods, cosmetics, pharmaceuticals, and agricultural products [1,2]. In most emulsions, the sizes of the droplets of the dispersed phase range from submicrometer to several micrometers. In contrast to microemulsions which are thermodynamically stable, emulsions are inherently unstable. However, by appropriately choosing the surfactant, which adsorbs on the interface between the two immiscible liquids, and stabilizes the droplets, emulsions can be kinetically stable nearly indefinitely, allowing their properties to be studied.

Emulsions exhibit many properties similar to those of dispersions of solid particles. The droplets of the dispersed phase execute Brownian motion in the fluid and the viscosity of the dispersion increases with their volume fraction. However, the physical properties of the interface are quite different; liquid droplets are flexible and their interfaces are therefore subject to thermal fluctuations. As a result, the shape of the droplets fluctuates and is itself a dynamic variable. The extra degree of freedom introduced by thermal shape fluctuations may have significant consequences for the properties of the emulsion; in particular, as the volume fraction ϕ is increased, the interaction between droplets may change because of this extra degree of freedom, and this may be reflected in the macroscopic properties of the emulsion. Moreover, the physical properties of the interfaces directly impact the formation and stability of an emulsion. Thus to fully explore the differences between dispersions of solid particles and liquid droplets requires the study of the shape fluctuations of the emulsion droplets. This may lead to an improved understanding of the stability and rheological properties of emulsions.

Thermally induced fluctuations on interfaces between two fluids are the well known capillary waves. The amplitude of these capillary waves is controlled by the surface tension between the fluids, Γ, and is typically very small, of the order of 10 Å for the commonly encountered values of the surface tension. Nevertheless, for flat interfaces capillary waves have been observed using both light [3] and x-ray scattering [4]. Thermally excited capillary waves on the interface of liquid droplets are much more difficult to observe because of the more complex geometry and the possibility that the interfacial fluctuations are coupled to other degrees of freedom, such as the translational motion of the droplets. However, thermal interfacial fluctuations of dispersions of other flexible particles have been observed; for example, shape fluctuations of micelles and microemulsions have been studied with neutron spin echo measurements [5,6], while those of liquid membranes have been observed with x-ray scattering [7] and those of vesicles have been studied with direct space imaging [8]. These systems share a number of distinct features. They are all suspensions of self-assembled structures. As a result, the interfacial tension is essentially zero, so that shape fluctuations are typically much larger, and thus easier to observe. These fluctuations are controlled by the interfacial rigidity or bending energy rather than by interfacial tension; consequently, the structures fluctuate about nonspherical mean shapes.

Typically one has to treat these dynamics phenomenologically by defining a free energy of bending. Moreover, these structures themselves have finite lifetimes, so the dynamics of these systems can include the creation and destruction of the constituent structures. Each system exists only over certain ranges of dispersed phase and surfactant concentrations, so that the full range of dispersed-phase volume fraction is not accessible for study. By contrast, the constituent particles of an emulsion are fluid droplets with a spherical mean shape controlled by the surface tension. The relaxation of the shape fluctuations can be predicted by hydrodynamics; the value of the interfacial tension Γ can be determined from macroscopic measurements. Moreover, the volume fraction of the dispersed phase can be varied continuously from zero to almost 1, allowing the volume-fraction-dependent interactions to be studied. Thus emulsions are a useful model system for studying shape fluctuations of dispersions of flexible particles.

Despite the potential interest and importance in studying the shape fluctuations of emulsion droplets, there are significant experimental difficulties, which have prevented their observation, until recently two breakthroughs removed obstacles that have previously stood in the way of our observing and understanding the shape fluctuations of droplets in emulsions. The first obstacle is the requirement of monodisperse emulsion droplets; since the shape fluctuations and their dynamics depend on droplet size, a polydisperse emulsion would preclude any quantitative theoretical analysis. The second major obstacle is the very small amplitude and the rapid relaxation of thermal shape fluctuations of micrometer-sized liquid droplets whose shape is controlled by interfacial tension. The extra surface area created by thermal deformations from a spherical shape is $\Delta A \approx k_B T/\Gamma$, where k_B is Boltzmann's constant and T is the temperature. For a typical interfacial tension of $\Gamma = 10$ dyn/cm, this extra surface area is only about 40 Å^2. If the radius of the droplet is $R \approx 1$ μm, the extra surface area corresponds to a relative variance from the mean spherical shape of only $\sim 10^{-7}$. Moreover, the relaxation time τ of these fluctuations is also very short. If the viscosity of the liquid comprising the drop is much greater than that of the continuous phase, the relaxation time is given by $\tau \approx R\eta/\Gamma$; for $\eta = 10$ cP, $\tau \approx 10^{-6}$ sec. The combination of the very short time scale and very small amplitude of the thermal fluctuations of emulsion droplets presents an experimental challenge to their observation.

In this paper we present a detailed study of the thermally induced shape fluctuations of emulsion droplets. We overcome the two major experimental obstacles; we exploit a recently developed purification technique to obtain the requisite monodisperse droplets, and we generalize diffusing-wave spectroscopy (DWS) to probe the minute amplitude of the shape fluctuations. Diffusing-wave spectroscopy extends dynamic light scattering (DLS) to the high multiple scattering limit [9], and probes dynamics on length scales much shorter than the wavelength of the incident light, λ. Several detailed discussions about the theoretical underpinnings of DWS have recently been published [10,11]. To study shape fluctuations, we generalize the theory of DWS to account for the fluctuations in the scattering amplitude of each droplet that result from the fluctuations in its shape; this generalization can also apply more broadly to other kinds of fluctuations in the scattering amplitude. We analyze the dynamics of thermally excited shape fluctuations using a series expansion in spherical harmonics of shapes that differ only slightly from a sphere. Starting from the surface potential energy governing the dynamics, we compute the amplitudes and relaxation times of thermally induced shape fluctuations controlled by surface tension. The experimental data from DWS measurements are inverted and analyzed with the generalized theory, enabling us to clearly resolve the shape fluctuations. Excellent agreement between our experimental data and theoretical prediction is found in the limit of low droplet volume fraction ϕ. Moreover, for the data at higher ϕ, a surprising scaling behavior is found enabling the data for all volume fractions over the range of liquidlike emulsions to be collapsed onto the curve predicted for low ϕ. We find that the characteristic decay rate of the shape fluctuations decreases linearly with increasing ϕ, while their amplitude increases. We discuss the possible origin of this behavior. Shape fluctuations persist even in compressed emulsions, i.e., emulsions with ϕ above hard-sphere close-packing values. We give a more qualitative discussion of their behavior.

The remainder of this paper is arranged as follows. In the next section, we generalize the theory for DWS by including the consequences of fluctuations of the scattering amplitude in the calculation of the temporal correlation function of the scattered electric field. In Sec. III, we analyze the scattering amplitude fluctuations that are caused by thermally induced shape fluctuations of particles whose shape is controlled by surface tension. Section IV contains a brief description of the preparation of monodisperse emulsions and the experimental details of the DWS measurements. In Sec. V, we present our experimental results. The consequences of the interactions between droplets are discussed and a simple model is proposed to attempt to interpret the volume fraction dependence. Concluding remarks are presented in Sec. VI.

II. DIFFUSING-WAVE SPECTROSCOPY WITH FORM FACTOR FLUCTUATIONS

In order to interpret quantitatively any results obtained with a DWS experiment, we must calculate the temporal autocorrelation function of intensity fluctuations of the scattered light. For all DWS experiments this is calculated by dividing the photons into separate, diffusive paths, each containing a large number of scattering events. The probability that a photon will follow a path of length s is determined through the use of the diffusion equation for the light solved for the experimental geometry. The correlation function for each such path is calculated by assuming that the path is comprised of a sequence of $n = s/l$ scattering events, where l is the scattering mean free path. Since n is typically large, each scattering event is assumed to be independent, and thus may be treated as the average scattering event; the aver-

age is taken over all possible scattering wave vectors $\mathbf{q}$. To utilize the diffusion approximation for the transport of the light, the number of scattering events must be expressed in terms of the transport mean free path l^*, the only length scale appropriate for diffusive light. The total correlation function is determined by summing the contributions of all possible paths, weighted by their probabilities. If the positions of the scattering particles in each path are completely uncorrelated, we need to consider only the contributions of individual paths; these can be added, assuming that all interference that contributes to the final signal comes only outside the sample, at the detector. If the scattering from some of the particles is strongly correlated, we need to consider the possible correlations of different scattering particles; this has been done in the case of scattering from solid sphere dispersions [12–15].

All these analyses of the DWS correlation functions assume that the fluctuations arise exclusively from the translational motion of the scatterers. This results in fluctuations of the phase of the light, which are detected through the interference with the light from other paths. To incorporate the effects of shape fluctuations, we must also allow the scattering intensity from each particle to fluctuate; this will result in intensity fluctuations that occur independently from any phase fluctuations. Thus the intensity of the light scattered from a suspension of droplets fluctuates not only because of the fluctuating phase interferences among the fields scattered by pairs of droplets as they execute relative translational motions, but also because of the fluctuating amplitude of the field scattered by each individual droplet. The time-dependent amplitudes of the scattered fields reflect the shape fluctuations. To account for these shape fluctuations, we assume that, aside from constants which disappear through later normalization, the field scattered from a liquid droplet can be written as

$$E_i(q,t)=[b_i(q)+\Delta b_i(q,t)]\exp\{i\mathbf{q}\cdot\mathbf{r}_i(t)\} \ . \tag{1}$$

Here $\mathbf{q}$ is the scattering wave vector, $\mathbf{r}_i(t)$ is the position of the center of mass of droplet i at time t, $b_i(q)$ is the average field amplitude from an individual scatterer, and $\Delta b_i(q,t)$ is the fluctuating part of the amplitude which depends on the instantaneous geometry of the scatterer.

The contribution from each independent scattering event in a DWS experiment can be expressed in terms of the dynamic structure factor, to reflect the correlations of particles inherent in a concentrated suspension [12–15]. Here we must generalize the expression given there to include the fluctuating portion of the scattering amplitude. Our goal is to obtain an expression for $g_1^n(t)$, the correlation function of the field scattered by a path with n scattering events, where we have recast the contribution of the amplitude fluctuations in the same functional form as the contribution of translational motions. This will allow us to adopt directly all the formalism for constructing the full correlation function in terms of the diffusion approximation for the transport of the light. Thus the autocorrelation function of the scattered field when only single scattering events occur is

$$\langle E^*(q,0)E(q,t)\rangle=\left\langle \sum_i \sum_j [b_i(q)+\Delta b_i(q,0)] \times[b_j(q)+\Delta b_j(q,t)] \times e^{i\mathbf{q}\cdot[\mathbf{r}_j(t)-\mathbf{r}_i(0)]}\right\rangle . \tag{2}$$

For monodisperse particles the average scattering amplitudes are the same, so that $b_i(q)=b_j(q)=b(q)$. Furthermore, we assume that the fluctuating scattered amplitude from one drop is uncorrelated with that of other drops, or with the average amplitude. Thus,

$$\langle b_i(q)\Delta b_j(q,t)\rangle=0 \ , \tag{3a}$$

$$\langle \Delta b_i(q,0)\Delta b_j(q,t)\rangle=0, \quad i\neq j \ , \tag{3b}$$

$$\Delta b_i(q,0)\Delta b_i(q,t)\rangle=\Delta F(q,t) \ , \tag{3c}$$

where $\Delta F(q,t)$ is the fluctuating portion of the scatterer form factor. Since $b_i(q)$ is a nonfluctuating quantity, the implication of Eq. (3a) is that $\Delta b_i(q,t)$ has zero mean. The average form factor is given by

$$F(q)=[b(q)]^2 \ . \tag{4}$$

In the absence of fluctuations of the form factor, the correlation function reduces to the familiar form,

$$\langle E^*(q,0)E(q,t)\rangle=NF(q)S(q,t) \ , \tag{5}$$

where the dynamic structure factor is given by

$$S(q,t)=\frac{1}{N}\left\langle \sum_i \sum_j e^{i\mathbf{q}\cdot[\mathbf{r}_j(t)-\mathbf{r}_i(0)]}\right\rangle , \tag{6}$$

where the angular brackets indicate an average over all ensembles of scatterers. In the absence of correlation between particles, the terms with $i\neq j$ do not contribute and Eq. (6) reduces to the self-dynamic structure factor

$$S_s(q,t)=\frac{1}{N}\left\langle \sum_i e^{i\mathbf{q}\cdot\Delta\mathbf{r}_i(t)}\right\rangle , \tag{7}$$

which describes single particle motion.

Including the fluctuations in the form factor, the field correlation function becomes

$$\langle E^*(q,0)E(q,t)\rangle=NF(q)S(q,t)+N\Delta F(q,t)S_s(q,t) \ , \tag{8}$$

where the second term in the autocorrelation function is just the time-dependent part of the scattering form factor multiplied by the *self-dynamic structure factor* and reflects the contribution of the shape fluctuations.

In DWS we measure dynamics on short length scales which typically correspond to short time dynamics. We can therefore approximate the full and self-dynamic structure factors by their behavior at short times. We write [12,14]

$$S(q,t)=S(q)\left[1-q^2D_0\frac{H(q,t)}{S(q)}t\right] , \tag{9}$$

where $D_0=k_BT/6\pi\eta a$ is the self-diffusion coefficient of

an isolated sphere of radius a in a fluid of viscosity η, and

$$H(q,t)=\frac{1}{2D_0 t}\left\langle \frac{1}{N}\sum_{i,j=1}^{N}\hat{\mathbf{q}}\cdot\Delta\mathbf{r}_i(t)\hat{\mathbf{q}}\cdot\Delta\mathbf{r}_j(t)e^{i\mathbf{q}\cdot\Delta\mathbf{r}_{ij}}\right\rangle , \tag{10}$$

which accounts for the hydrodynamic interactions between the particles. In the absence of correlations, the self-dynamic structure factor becomes

$$S_s(q,t)=1-\frac{q^2}{6}\langle\Delta r^2(t)\rangle , \tag{11}$$

reflecting the mean-square displacement of the particles. To obtain the average single scattering correlation function required for the construction of the DWS correlation function, we must average Eq. (8) over all possible angles. We transform the average over angles into an integral over $\mathbf{q}$, obtaining

$$\begin{aligned}\langle E^*(q,0)E(q,t)\rangle_q &= N[\int F(q)S(q)q\,dq-\int q^3F(q)H(q)dq\,D_0t \\ &\quad+\int\Delta F(q,t)q\,dq] ,\end{aligned} \tag{12}$$

where we have ignored the second order small quantity $(q^2/6)\Delta r^2(t)\Delta F(q,t)$, with the assumption $\Delta F(q,t)\ll F(q)$. To calculate $g_1^n(t)$, the contribution to the DWS correlation function from a path with n scattering events, we assume that each scattering event is independent and take the product of n q-averaged single scattering correlation functions and normalize by the value at $t=0$,

$$g_1^n(t)=\frac{\langle E^*(q,0)E(q,t)\rangle_q^n}{\langle E^*(q,0)E(q,0)\rangle_q^n} . \tag{13}$$

Keeping only the first order terms,

$$\begin{aligned}g_1^n(t)&=1-n\frac{\int q^3F(q)H(q,t)dq}{\int qF(q)S(q)dq}D_0t \\ &\quad-n\frac{\int qF(q,0)dq-\int qF(q,t)dq}{\int qF(q)S(q)dq} ,\end{aligned} \tag{14}$$

where $S(q)$ is the static structure factor, or $S(q,t)$ evaluated at $t=0$. Equation (14) can be approximated as

$$\begin{aligned}g_1^n(t)=\exp\left\{-n\frac{\int q^3F(q)H(q,t)dq}{\int F(q)S(q)q\,dq}D_0t\right. \\ \left.-n\frac{\int\Delta F(q,0)q\,dq-\int\Delta F(q,t)q\,dq}{\int F(q)S(q)q\,dq}\right\} ,\end{aligned} \tag{15}$$

since $\int q^3F(q)H(q,t)dq\,D_0t$ and $\int\Delta F(q,t)q\,dq \ll\int F(q)S(q)q\,dq$. This approximation expresses the q-averaged, n-event scattering field correlation function as the exponential of a time-dependent function. This is the same form that arises in the treatment of systems that have only translation dynamics. Thus we have incorporated amplitude fluctuations in the desired form.

To use the diffusion approximation for light propagation through the medium, we describe the diffusive step length l of the diffusing light in terms of the transport mean free path l^*, which is defined by [16]

$$\frac{l^*}{l}=\frac{2k_0^2\int qF(q)S(q)dq}{\int q^3F(q)S(q)dq} , \tag{16}$$

where k_0 is the wave number of the light in the continuous phase of the emulsion. The number of scattering events can then be expressed in terms of the path length normalized by the transport mean free path, $n=(s/l^*)(l^*/l)$, where Eq. (16) is used for the factor l^*/l. We introduce the notation

$$[S]=\frac{\int q^3F(q)S(q)dq}{\int q^3F(q)dq} , \tag{17}$$

which is the structure factor as averaged in a DWS experiment, and

$$[H]=\frac{\int q^3F(q)H(q,t)dq}{\int q^3F(q)dq} , \tag{18}$$

which is the similarly averaged hydrodynamic interaction factor. We note here that the DWS average includes a weighting by $q^3F(q)$ and strongly emphasizes the high-q region of both $S(q)$ and $H(q,t)$.

The DWS q averages are equivalent to averages over scattering angles. Also $F(q)$ is proportional to the differential cross section $d\sigma_0/d\Omega$ associated with the time-averaged particle shape, while $\Delta F(q,t)$ is proportional, via the same constant, to the autocorrelation function of the fluctuating part of the square root of the cross section of the fluctuating shape. We therefore define

$$\sigma_0=\int F(q)q\,dq , \tag{19}$$

$$\Delta\sigma(t)=\int\Delta F(q,t)q\,dq . \tag{20}$$

We shall show that the DWS measurement is sensitive to the ratio $\Delta\sigma(t)/\sigma_0$; we therefore ignore the common proportionality constant and refer to σ_0 as the equilibrium total cross section and $\Delta\sigma(t)$ as the total cross section deviation function.

Introducing these definitions into Eq. (15), we express the correlation function for the field scattered from a path of length s as

$$\begin{aligned}g_1^s(t)=\exp\left\{-\frac{2k_0^2s}{l^*[S]}\left[[H]D_0t\right.\right. \\ \left.\left.+\frac{l_0^*}{2k_0^2l_0}\frac{\Delta\sigma(0)-\Delta\sigma(t)}{\sigma_0}\right]\right\} .\end{aligned} \tag{21}$$

The first term in the exponent is identical to the expression obtained in the absence of amplitude fluctuations,

while the second term reflects the effects of the amplitude fluctuations. The quantity l_0^*/l_0 is defined by Eq. (16) with $S(q)$ set equal to 1. It may be interpreted as the ratio of the transport and scattering mean free paths for light diffusing through a suspension of scatterers among which there are no spatial correlations, and reflects our assumption that the shape fluctuations of one droplet are uncorrelated with those of any other droplet. Thus the shape fluctuations result in a contribution to the correlation function that adds to the contribution of translational motions. The shape fluctuation contribution increases from zero and saturates at a value proportional to $\Delta\sigma(0)/\sigma_0$, reflecting the relaxation of deformed shapes. Because the shape fluctuation contribution is additive, it competes with the contribution of translational motion; as a result, it should be observable only if shape deformations relax in less time than is required for significant translational motions. The full DWS correlation function is obtained by summing over all paths, weighted by the probability $P(s)$ that a photon follows a path of lengths s:

$$g_1(t)=\int P(s)\exp\left\{-\frac{2k_0^2 s}{l^*[S]}\left[[H]D_0 t+\frac{l_0^*}{2k_0^2 l_0}\frac{\Delta\sigma(0)-\Delta\sigma(t)}{\sigma_0}\right]\right\}ds\ . \tag{22}$$

We note that the autocorrelation function resembles the Laplace transform of the probability distribution function $P(s)$. The quantity $P(s)$ depends explicitly on the shape and illumination of the scattering cell. We determine it for any given experimental geometry by solving the diffusion equation with appropriate boundary conditions [9,11]. The transport mean free path l^* and the DWS-averaged structure factor $[S]$ can also be measured or calculated independently of the measurement of $g_1(t)$. The right side of Eq. (22) is therefore a known function of the quantity in square brackets. From a tabulation of this function and the measured value of g_1 at a given time t, we are thus able to obtain the value of the quantity in square brackets at time t. We refer to this procedure as the inversion of the DWS correlation function; this inversion is unrelated to Laplace transform inversion. The first term in the square brackets describes the contribution to the correlation decay from the apparent diffusion. Collective effects in these translational motions are described by $[H]$. For the case of relatively large particles satisfying $R \geq \lambda$, the high-q weighting of the DWS averages allows us to approximate $[H]D_0 t$ as $\langle \Delta r^2(t)\rangle/6$. In this case DWS probes the mean-square displacement $\langle \Delta r^2(t)\rangle$ [11]. The second term contains the effects of the amplitude fluctuations. Its prefactor l_0^*/l_0 must be evaluated in the limit of zero volume fraction and has no volume fraction dependence. It is clear from Eq. (22) that DWS probes the relative fluctuations of the cross section. Like $\langle \Delta r^2(t)\rangle$, their contribution to the decay of $g_1(t)$ increases from zero at $t=0$, but it saturates at long times, while $\langle \Delta r^2(t)\rangle$ and its contribution continue to increase. It is also clear why very small motions can be detected with DWS: for long paths, $s/l^* \gg 1$; this large factor in Eq. (22) allows small values of the quantity in the square brackets to contribute to the decay of $g_1(t)$. The signal arises from the sum of a large number of independent amplitude fluctuations. They would not be detectable without the advantage of multiple scattering.

We note that the derivation is independent of the nature of the amplitude fluctuations; not only shape fluctuations but other phenomena, such as rotational motion of aspherical particles, can also result in a similar contribution.

III. DYNAMICS OF SHAPE FLUCTUATIONS OF EMULSION DROPLETS

The fluctuations in the shape of an emulsion droplet result from capillary waves on its interface. Their amplitudes are determined by the thermal energy which excites them and by the interfacial tension Γ which controls them. A change in shape results in an increase of the interfacial area ΔA, and therefore an increase of the surface potential energy. Since the fluids are incompressible, the droplet volume remains fixed, and a change in surface area results in a change in shape. The thermal energy $k_B T$ is much less than the total surface potential energy ΓR^2, so $k_B T \approx \Gamma \Delta R^2 \ll \Gamma R^2$. We must calculate the fluctuating shape of the droplets due to the thermally excited capillary waves, and the scattering cross section of this fluctuating shape.

To calculate the fluctuating shape, we express the surface potential energy as a sum of spherical harmonics and use the equipartition theorem to assign each mode an energy of $k_B T/2$. Because of thermal excitation, the liquid drop has at any instant a nonspherical shape. The surface potential energy E can be written as

$$E=\Gamma A=\Gamma\int_0^{\pi 2}\int_0^{\pi}\left[r^2+\frac{1}{2}\left[\frac{\partial r}{\partial\theta}\right]^2+\frac{1}{2\sin^2\theta}\left[\frac{\partial r}{\partial\varphi}\right]^2\right]\sin\theta\, d\theta\, d\varphi\ , \tag{23}$$

where we take the surface tension Γ as a constant, by assuming the fluctuating amplitude is small so that the effect of surface dilation on Γ is negligible. Here A is the surface area of the distorted sphere and $r(\theta,\varphi,t)$ is its instantaneous radius as a function of polar angles θ and φ. We expand $r(\theta,\varphi,t)$ in a series of spherical harmonics $Y_{lm}(\theta,\varphi)$ [5,6,17],

$$r(\theta,\varphi,t)=r_0\left[1+\sum_{l=2}^{l_{\max}}\sum_{m=-1}^{m=1}a_{lm}(t)Y_{lm}(\theta,\varphi)\right], \tag{24}$$

where $l=0$ and $l=1$ are excluded because they represent

a dilation and translation of the drop, and where r_0 is the zeroth order term in the expansion. Thus the surface energy is

$$E=4\pi\Gamma r_0^2\left[1+\frac{1}{8\pi}\sum_{l=2}^{l_{\max}}\sum_{m=-l}^{m=l}(-1)^m[l(l+1)+2]\times a_{lm}a_{l,-m}\right]. \quad (25)$$

Since the volume is conserved,

$$\frac{4\pi}{3}R^3=\int\int\tfrac{1}{3}[r(\theta,\varphi)]^3\sin\theta\,d\theta\,d\varphi\ , \quad (26)$$

where R is the radius of the undistorted spherical droplet. Neglecting higher order terms, we can determine the first order term, using the constraint of Eq. (26),

$$r_0=R\left[1-\frac{1}{4\pi}\sum_{l=2}\sum_{m=-l}^{m=l}a_{lm}a_{l,-m}(-1)^m\right]. \quad (27)$$

Then, the expression for the potential energy becomes

$$E=4\pi\Gamma R^2\left[1+\frac{1}{8\pi}\sum_{l=2}^{l_{\max}}\sum_{m=-l}^{m=l}[l(l+1)-2]|a_{lm}|^2\right]. \quad (28)$$

Here we have an excess surface free energy because of shape fluctuations. According to the equipartition principle, we take the ensemble average of Eq. (28) and give each mode an energy of $\frac{1}{2}k_BT$ to obtain the mean-square amplitude of each mode,

$$\langle|a_{lm}|^2\rangle=\frac{k_BT}{\Gamma R^2}\frac{1}{l(l+1)-2}\ . \quad (29)$$

In the case of an emulsion system, the shape fluctuations for each mode take place at low Reynolds number, where convective and inertial terms in the Navier-Stokes equations can be neglected [18]. The differences in the normal components of the viscous stresses are balanced by the Laplace pressure of the deformed surface and the fluid velocities are continuous. These boundary conditions determine the relaxation of the deformed droplet to spherical shape. Thus, in this overdamped limit, the autocorrelation function of the fluctuating amplitude is given by

$$\langle a_{lm}^*(0)a_{l'm'}(t)\rangle=\frac{k_BT}{\Gamma R^2}\frac{\delta_{ll'}\delta_{mm'}}{l(l+1)-2}e^{-\omega_l t}\ , \quad (30)$$

where the decay rate for modes l is given by [19]

$$\omega_l=\frac{l(l+2)(2l+1)}{2(2l^2+4l+3)}\frac{\Gamma}{\eta R}\ . \quad (31)$$

In general, ω_l depends on the viscosities of both fluids [20]; we have assumed that the viscosity η of the interior is much greater than that of the surrounding fluid. We note that asymptotically $\omega_l\sim l$, reflecting the fact that the dynamics are controlled by surface tension; by contrast, $\omega_l\sim l^3$ when the dynamics are controlled by the interfacial rigidity [17].

To calculate the far field scattering amplitude from these shape fluctuations, $b(q,t)$, we should use the exact Mie scattering theory [21], suitably generalized to treat nonspherical scatterers. But as a first approximation we restrict the calculation to the dipole contribution, using the Rayleigh-Gans (RG) approximation [21]. We recognize that this is not strictly correct, and test the errors introduced by this approximation later. The instantaneous scattering amplitude $b(q,t)$ can be expressed as

$$b(q,t)=\frac{1}{V}\int_V e^{i\mathbf{q}\cdot\boldsymbol{\rho}'}d^3\rho' \quad (32)$$

where $\mathbf{q}$ is the scattering vector, V is the volume of the scatterer, and the integration vector $\boldsymbol{\rho}'$ connects the origin with a point inside the scatterer. The upper limit $\rho_{\max}$ for its magnitude is just the instantaneous, direction-dependent radius of the droplet, which we express as a series expansion of spherical harmonics

$$\rho_{\max}(\theta,\varphi)=R\left[1+\sum_{l=2}^{l=l_{\max}}\sum_{m=l}^{m=-l}a_{lm}Y_{lm}(\theta,\varphi)\right], \quad (33)$$

where we now neglect the distinction between R and r_0 and a_{lm} are expansion coefficients whose autocorrelators have been determined in Eq. (30).

The plane wave in Eq. (32) can also be expressed as a series expansion:

$$e^{iq\rho'\cos\gamma}=\sum_{l=0}^{\infty}(2l+1)i^l j_l(q\rho')P_l(\cos\gamma)\ , \quad (34)$$

where $j_l(q\rho')$ and $P_l(\cos\gamma)$ are the lth order spherical Bessel function and Legendre polynomial, and γ is the angle between the scattering vector $\mathbf{q}$ and the integration vector $\boldsymbol{\rho}'$. Completing the integration of Eq. (32), we arrive at the time-dependent form factor $F(q,t)$ which is the autocorrelation function of the scattering amplitude [5]:

$$F(q,t)=\langle b^*(q,0)b(q,t)\rangle=\left[\frac{3j_1(qR)}{qR}\right]^2+\frac{1}{4\pi}\sum_{l=2}(2l+1)[3j_l(qR)]^2\langle a_l^*(0)a_l(t)\rangle\ . \quad (35)$$

A DWS experiment probes the q-averaged form factor. Thus we integrate Eq. (35) over q, obtaining the total scattering cross section, apart from a constant prefactor depending on the relative refractive index which we may omit since we are concerned with the ratio of the fluctuating and constant parts of the cross section. Apart from the prefactor, the cross section consists of the constant part σ_0 and the time-dependent part $\Delta\sigma(t)$, defined previously by Eqs. (19) and (20). Within the RG approximation, the explicit expressions are

$$\sigma_0=\pi\int_0^{\pi}(1+\cos^2\theta)\left[\frac{3j_1(qR)}{qR}\right]^2\sin\theta\,d\theta \quad (36)$$

and

$$\Delta\sigma(t)=\frac{k_BT}{4\pi\Gamma R^2}\sum_{l=2}\frac{2l+1}{l(l+1)-2}g_l\exp(-\omega_l t)\ , \quad (37)$$

where g_l is given by

$$g_l = \pi \int_0^{\pi} (1+\cos^2\theta)[3j_l(qR)]^2 \sin\theta \, d\theta \ . \quad (38)$$

In Eqs. (36) and (38), the scattering wave number is $q = 2k_0 \sin(\theta/2)$, where k_0 is the wave number of the incident radiation in the continuous phase of the emulsion. The factor $1+\cos^2\theta$ is appropriate for an unpolarized incident beam [21] and reflects the effect that multiply scattered light is completely depolarized. The coefficients g_l depend only on k_0R and express the scattering efficiency of each deformation mode. They become negligible when $l \gg k_0R$, since the length scale of the features described by such modes is much smaller than the wavelength of the radiation. This behavior of g_l makes the assignment of a cutoff mode number unnecessary in Eq. (37), although such a cutoff $l_{\max}$ is required in Eq. (25) to avoid a logarithmic divergence of the surface energy E. Thus, for a given droplet size and laser wavelength, only a finite number of modes contribute to the scattering. For example, we find that the series converges for $l \approx 20$ for a 1.4 μm diameter droplet and $k_0 = 16.3\ \mu\text{m}^{-1}$. Note that Eqs. (36) and (37) define σ_0 and $\Delta\sigma(t)$ as dimensionless quantities: here we neglect a common prefactor that differs from the one we neglected in Eqs. (19) and (20). The ratio is, of course, not affected.

Because of the large refractive index mismatch Δn between oil and water, the criterion $\Delta n k_0 R \ll 1$ for the validity of the Rayleigh-Gans approximation does not strictly hold for an emulsion droplet. Nevertheless, it appears that the RG theory is sufficiently accurate to describe our system. We arrive at this conclusion by calculating with the Mie theory the exact form factor of an undeformed sphere and comparing the result with that found from the RG theory. Thus, a calculation of the constant part of the total cross section in absolute units yields $\sigma_0 = 0.995\ \mu\text{m}^2$ from Mie theory and $0.999\ \mu\text{m}^2$ from RG theory. Moreover, we also use the exact calculation for spheres in an *ad hoc* procedure that tests the accuracy with which the RG theory determines the scattering power of nonspherical shapes. To accomplish this, we use identities satisfied by Bessel functions to rewrite Eq. (38) for the dominant coefficient g_2, which describes the scattering from ellipsoidal deformations, in terms of the derivative with respect to qR of the form factor of an undeformed sphere. We then use the Mie theory to evaluate this form factor and its derivative exactly. We find that the values obtained by this method and by direct evaluation of Eq. (38) agree to about 10%, the value directly predicted by the RG theory being the lower of the two. Thus we conclude that applying the RG theory to our scattering measurements allows us to infer the essential behavior of shape fluctuations, with an uncertainty of about 10%. Hereafter, we use the Rayleigh-Gans approximation exclusively, since it allows us to directly evaluate the contribution to the correlation function due to shape fluctuations through Eqs. (31) and (36)–(38).

IV. EXPERIMENTAL METHOD

Our emulsion samples are three-component suspensions consisting of dispersed oil, continuous water, and sodium dodecylsulfate (SDS) surfactant on the interfaces. The SDS surfactant molecules play two roles in the emulsification process. First, they lower the interfacial tension and thereby make it easy to create small droplets. Second, they stabilize the dispersed droplets against coalescence once they are formed. Mechanical energy is added to the three-component system by mixing oil, water, and surfactant with a Kitchen Aid mixer. The ratio of the three components is adjusted to facilitate the formation of emulsions. The peak of the size distribution of the emulsion droplets can be controlled by varying the mixing time and the shear rate exerted by the mixer. Crude emulsions with droplet sizes ranging from 0.1 to 2 μm are first prepared in highly concentrated form. The polydisperse emulsions are purified with the technique of fractionated crystallization, which is based on the liquid-solid phase transition induced by the attractive depletion interaction. The attractive interaction between the droplets arises from the noncompensated pressure exerted by surfactant micelles in the suspension. The detailed purification principles have been summarized in the literature [22]. By adjusting the micelle concentration we obtain highly monodisperse emulsions after eight steps of the purification process. The polydispersity is about 6% of the average radius, and is sufficiently low that the samples form colloidal crystals, analogous to hard-sphere dispersions at appropriate volume fractions [23]. Because the droplets are deformable, their volume fraction can be increased to well above hard-sphere close-packing values. This is accomplished by putting the emulsion in a dialysis bag, which is immersed in a large reservoir containing water, sodium dodecyl sulfate detergent (SDS), and a hydrophilic polymer, dextran, with molecular weight (MW) of 500 000. Dextran is chosen because the osmotic pressure and surfactant chemical potential can be independently controlled in a SDS-dextran-water mixture by varying the polymer concentration and surfactant concentration. The dialysis bag is made of a cellulosic membrane with a MW cutoff of 50 000. It is permeable to water and surfactant, but impermeable to the oil droplets and polymer. Thus, taking advantage of the osmotic pressure, we can increase the volume fraction by pumping the excess water out of the bag. Then the volume fraction is measured directly by weighing a portion of sample before and after drying in a vacuum oven, maintained at room temperature. The weight fractions are converted to volume fractions under the assumption that the density of the droplets is the same as the density of the bulk oil. This enables us to study the effects of the volume fraction of the droplets on their shape fluctuations.

The standard experimental setup for DWS in transmission is used [15]. The beam from an Ar^+ laser is focused on one side of the sample cell containing the emulsion, and scattered light is collected from the other side. The Ar^+ laser operates in a single longitudinal mode at a wavelength of 514.5 nm in vacuum. Single mode operation is essential because our detection system is sufficiently fast to be able to detect the beats between neighboring longitudinal modes of the laser, which occur at 125 MHz. Moreover, operating in a single mode en-

sures that the coherence length of the light is larger than the longest diffusive light paths in the sample.

To enable us to study the very fast phenomena of interest, we use a cross-correlation technique. The scattered light is divided into two equal portions and is detected with two photomultiplier tubes (PMT's). The outputs of these are cross correlated. This method reduces the deleterious effects of afterpulsing in the individual PMT's, which otherwise introduce a spurious correlation at short times. The cross-correlation technique also reduces the effects of dead times in the PMT's and counting electronics, and, provided that the count rate in each tube is not too large, allows measurements at faster time scales.

Our detection optics are optical fibers. We use two different types, single mode and multimode. In both cases, the beam splitter is integrated into the fibers, greatly simplifying the alignment. The multimode fiber has a core diameter of 100 μm, and standard two-pinhole optics are used to collect the light. A lens is used to image the fiber face onto the face of the sample and an aperture at the lens is adjusted to limit the range of scattering vectors collected by the fiber core, which serves as the second pinhole. In the case of a single mode fiber, the light is collected by a graded index (GRIN) lens of 0.25 pitch, which is integrated on the fiber cable. The single mode fiber collects only the light incident on the face of the GRIN lens which is of a single spatial mode. This arrangement results in a much higher spatial coherence factor, while maintaining a high light-collecting efficiency [24]. Moreover, the single mode fiber receiver offers the possibility of working with an arbitrarily large scattering volume and with an arbitrary working distance.

Like all forms of dynamic light scattering, a DWS experiments measures the temporal autocorrelation function of the fluctuations of the scattered light intensity. The intensity correlation function is related to the field correlation function through the Siegert relationship

$$g_2(t)=1+\beta|g_1(t)|^2 . \tag{39}$$

The spatial coherence factor β depends on the number of coherence areas detected by the optics. The use of the Siegert relation is justified in DWS because the scattering volume—essentially the entire sample—is always much larger than the size of coherent structures within the system.

The scattering system here consists of liquid oil droplets dispersed in water. The average radius of the oil droplets is $R=0.7$ μm. The polydispersity (normalized rms radius deviation) is about 6%. The index of refraction of the oil is 1.401; since the refractive index of water n is 1.33, the system scatters light very strongly. With the volume fraction above 5% and the sample cell thickness of 4 mm, the high multiple scattering limit can easily be reached in the transmission geometry. Similar emulsions were prepared from oils of two different viscosities, $\eta=12$ and 1000 cP.

V. EXPERIMENTAL RESULTS

A typical autocorrelation function from the emulsion with the 12 cP oil is shown in Fig. 1. The data are obtained using an emulsion with $\phi=0.35$, and they have been normalized with the background subtracted, so that we plot $|g_1(t)|^2$. Only the initial decay is shown, to emphasize the deviation of the data from the behavior expected for a suspension of solid spheres at the same volume fraction. The behavior expected for hard spheres can be predicted from the measured scaling form [15], and is shown by the solid line. The data clearly deviate from the expected behavior; similar deviation is observed at all volume fractions. By contrast, the correlation function from an identical emulsion made from 1000 cP oil does agree very well with the prediction for solid spheres, as shown in Fig. 2. Moreover, similar good agreement is observed for initial decay of the correlation function for all volume fractions of this emulsion up to $\phi=0.45$.

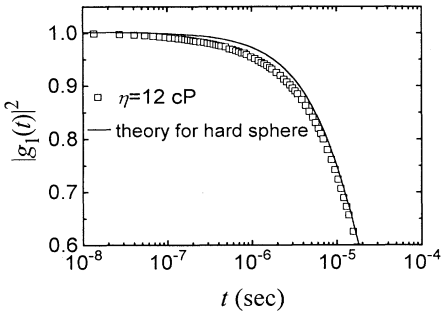

FIG. 1. The square of the normalized field correlation function $|g_1(t)|^2$ as measured by DWS for an emulsion of a low viscosity oil at volume fraction $\phi=0.35$. The smooth curve shows the theoretical behavior of a dispersion of hard spheres. The deviations of the data from the curve are caused by thermal shape fluctuations of the emulsion droplets.

The origin of the discrepancy is the fluctuations in the shape of the emulsion droplets. Their relaxation rate scales with the viscosity of oil; for droplets with higher viscosity, this relaxation rate is so slow that the decay of the correlation function is dominated by the translational motion of the droplets, so the shape fluctuations cannot be distinguished. By contrast, for the droplets with the low viscosity, the shape fluctuations relax sufficiently rap-

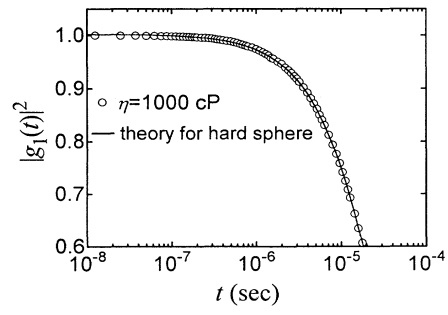

FIG. 2. The same as Fig. 1 for an identical emulsion of a high viscosity oil. Shape fluctuations are no longer visible because they occur on a longer time scale where dephasing by translations dominates the decay of $|g_1(t)|^2$.

idly that they can be clearly distinguished from the translational motion of the droplets.

To analyze the dynamics of the shape fluctuations, we invert the DWS intensity autocorrelation function as described in Sec. II and so obtain the quantity appearing in square brackets in Eq. (22). To set the absolute level of these data, we need to know the transport mean free path l^* and the DWS-averaged structure factor $[S]$. We evaluate $[S]$ from its definition [Eq. (17)], using the Mie theory to calculate the scattering form factor $F(q)$ and the expression for the total static structure factor for hard spheres $S(q,\phi)$ that is obtained with the Percus-Yevick approximation [25]. The value of l^* can, in principle, be obtained by two independent methods. It can be calculated from the Mie scattering theory with particle correlations taken into account through the use of a theoretical structure factor [16]. Alternatively, we can determine it experimentally by measuring the static transmission through the sample [9]. The static transmission is proportional to l^*; by comparing the measured transmission with that of a reference sample of identical thickness, and in the same optical configuration, we obtain the value of l^* relative to that of the reference sample. By using as a reference sample a hard-sphere suspension of relatively low volume fraction, we ensure that the reference value of l^* can be calculated with reasonable accuracy. Comparing the values we obtain for l^* using these two methods, we assign a 10% experimental uncertainty to the inverted correlation functions.

The inverted data for the two emulsions are plotted in Fig. 3, with open symbols used for the emulsion of 1000 cP oil and solid symbols used for the emulsion of 12 cP oil. The data consist of a sum of a contribution due to the translational portion, and another contribution due to the relaxation of the amplitude fluctuations $[\Delta\sigma(0)-\Delta\sigma(t)]/\sigma_0$. Since the droplets are relatively large, the translational contribution is given directly by the mean-square displacement $\langle\Delta r^2(t)\rangle$. As illustrated in Fig. 3, for the emulsion made of the high viscosity oil, the inverted data follow the curve predicted for solid spheres, shown by the solid line. In this case, the theory includes only the self-translational portion $\langle\Delta r^2(t)\rangle$, but incorporates the consequences of hydrodynamic interactions [15]. As probed by dynamic light scattering, the emulsion of the high viscosity oil is indistinguishable from a suspension of rigid spheres because here large translational displacements occur during the much longer relaxation time for shape fluctuations. The contribution from the shape fluctuations is therefore negligible in comparison with the contribution from translations. By contrast, an emulsion made of the lower viscosity oil exhibits distinct additional dynamics, shown by the solid circles in Fig. 3. At early times these data fall significantly above those of the heavy oil and those expected for solid spheres; at later times the data merge with the purely translational dynamics.

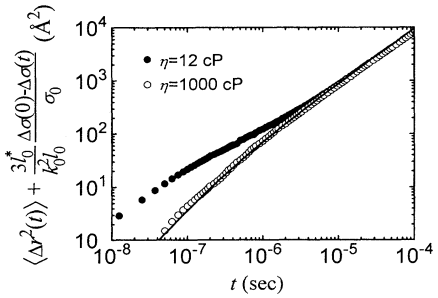

FIG. 3. The data of Figs. 1 and 2 in the inverted form discussed in the text. The data corresponding to the high viscosity oil (open circles) are well represented by the theoretical mean-square displacement $\langle\Delta r^2(t)\rangle$ of particles in a hard-sphere dispersion (smooth curve).

To investigate the relaxation of shape fluctuations more clearly, we separate the contributions of translational motion and shape fluctuations by subtracting the mean-square displacement from the inverted data. We can do this subtraction because the mean-square displacement can be calculated accurately: the prediffusional Brownian motion of an isolated particle has been calculated theoretically [26], while measurements performed on rigid hard spheres have established a scaling of the theory with volume fraction that accounts for interactions [13–15]. We plot $R^2\Delta\sigma(t)/\sigma_0$ for $\phi=0.35$ on a log-linear scale in Fig. 4; we multiply the normalized cross section deviation function $\Delta\sigma(t)/\sigma_0$ by R^2 since by doing so we obtain a quantity closely related to the autocorrelation function of fluctuations of the droplet radius. To establish this connection, we introduce here the radius correlation function of a fluctuating droplet using Eqs. (24) and (30),

$$\frac{1}{4\pi}\int\langle[r(0)-R][r(t)-R]\rangle d\Omega = \frac{k_BT}{4\pi\Gamma}\sum_{l=2}^{l_{\max}}\frac{2l+1}{l(l+1)-2}\exp(-\omega_l t)\ . \quad (40)$$

Comparing Eqs. (37) and (40), we see that the difference between the radius correlation function and $R^2\Delta\sigma(t)/\sigma_0$ is just the appearance in the latter of the coefficients g_l/σ_0 which characterize the scattering strength of each deformation mode relative to the scattering strength of the undeformed sphere. Hereafter we will call $R^2\Delta\sigma(t)/\sigma_0$ the shape fluctuation correlation function. It is the radius correlation function when the contributions of the deformation modes are taken with a scattered intensity weighting.

The curves shown in Fig. 4 have been calculated from Eqs. (36)–(38) together with overall rescalings of the amplitude and time scale, to be described below. For the dashed curve, we include only the first term, $l=2$, in the sum over deformation modes, resulting in a purely exponential decay. Comparison of this curve with the data makes evident the distinctly nonexponential relaxation of shape fluctuations. However, we obtain excellent agreement with the data when we include more modes, up to $l_{\max}=17$ (solid line). In a practical sense, the mode sum converges and the computed curve is insensitive to the value of $l_{\max}$ provided it is chosen larger than 10. On the other hand, the fit to the data is noticeably poorer if we choose $l_{\max}=5$ or less, indicating that higher order defor-

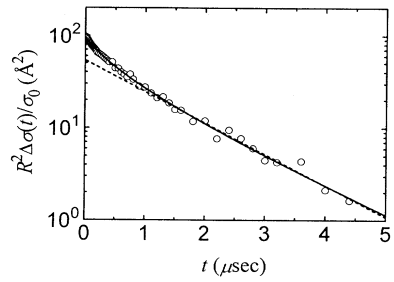

FIG. 4. Shape fluctuation correlation function of droplets in an emulsion of low viscosity oil at volume fraction $\phi=0.35$. The smooth curve is the theoretical prediction [Eqs. (36–38)], together with scalings of the amplitude and characteristic relaxation time as defined in the text. The dashed curve is the contribution from the dominant ($l=2$) mode alone.

mation modes contribute significantly.

In Fig. 5 we show logarithmic plots of the shape fluctuation correlation functions $R^2\Delta\sigma(t)/\sigma_0$ measured with emulsions whose droplet volume fractions cover the range $0.07<\phi<0.55$. The amplitudes of the shape fluctuations increase with ϕ. Figure 5 also shows the shape fluctuation correlation function of an isolated droplet as predicted by the theory without adjustments of any kind. The data appear to fall on curves which differ from the theoretical curve only by ϕ-dependent vertical and horizontal shifts. This surprising scaling behavior indicates that the relative strength and relaxation rates of the deformation modes of interacting droplets are the same as those of an isolated droplet. To test this suggestion, for each data set we scale the theoretical curve by treating as ϕ dependent two fitting parameters. These are the amplitude of the correlation function $R^2\Delta\sigma(t=0;\phi)/\sigma_0$, and the overall factor $\omega(\phi)$ that applies to the l-dependent mode relaxation rates ω_l. By comparison, the prediction of the theory for these parameters, for $\phi=0$, is

$$\frac{R^2\Delta\sigma(t=0;\phi=0)}{\sigma_0}=\frac{k_BT}{4\pi\Gamma\sigma_0}\sum_{l=2}g_l\frac{2l+1}{l(l+1)-2}=52\ \text{Å}^2 \tag{41}$$

and

$$\omega(\phi=0)=\frac{\Gamma}{\eta R}=1.2\times10^6\ \text{sec}^{-1}\ . \tag{42}$$

In Fig. 6 we plot the measured and theoretical shape fluctuation correlation functions, normalized by their fitted amplitudes to the theoretical amplitude of 52 Å^2, versus scaled time $\omega(\phi)t$. All the data do indeed collapse onto a single master curve. Furthermore, the measured data approach the theoretical curve given in Eqs. (36)–(38) as ϕ approaches zero: the extrapolation of the fitted $\omega(\phi)$ to $\phi=0$ gives a value identical to the predicted value of 1.2×10^6 sec^{-1}. Similarly the extrapolated value of the amplitude $R^2\Delta\sigma(t=0;\phi=0)/\sigma_0$ is 70 Å^2. The discrepancy with the predicted value 52 Å^2 may reflect the error introduced by the Rayleigh-Gans approximation, the error in our values for the scattering and transport mean free paths l and l^*, or the error incurred by our simple linear extrapolation of the amplitude–volume fraction relation defined by our two least concentrated samples.

To examine the ϕ dependence of shape fluctuations, we plot in Fig. 7 the relaxation rate scaling function $\omega(\phi)$, normalized by its theoretical value at $\phi=0$, 1.2×10^6 sec^{-1}. The normalized scaling function is well represented by $\omega(\phi)/\omega(0)=1-0.78\phi$. The ϕ dependence is relatively weak in the sense that there is no sign of the shape deformation relaxation rate extrapolating to zero as the volume fraction increases toward $\phi\approx0.63$, the value of random close packing of spheres, which is the limiting value for packing undeformed spheres; above this value, the droplets must be permanently deformed in order to pack together. The ϕ dependence is also linear, despite the high concentrations. Nevertheless, the behavior of the relaxation rate may be indirectly related to the ϕ dependence of the effective viscosity of the emulsion, even though the latter is strongly nonlinear over the volume fraction range our measurements cover. A similar linear form for the shape relaxation rate was recently predicted for the $l=2$ modes as part of a theory for the nonlinear ϕ dependence of the effective viscosity of a nondilute suspension of deformable droplets [27]. The predicted coefficient was 1.4, larger than the value 0.78

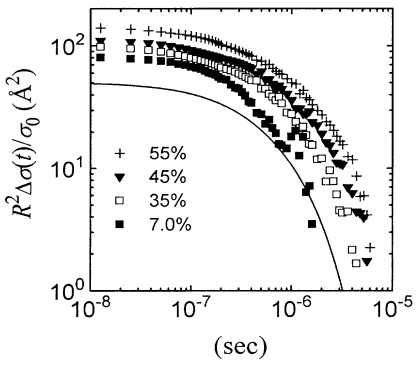

FIG. 5. Shape fluctuation correlation functions of droplets in emulsions covering a range of volume fractions. The smooth curve is the prediction of the theory without scalings.

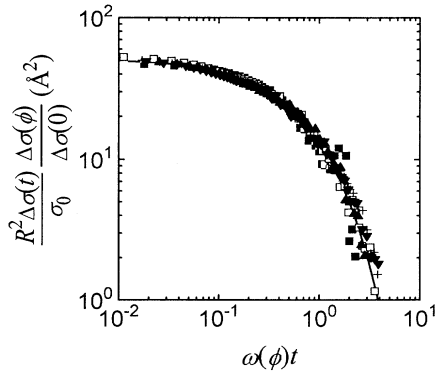

FIG. 6. The data of Fig. 5 in scaled form. The measured shape fluctuation correlation functions of interacting droplets collapse to a universal curve which is identical to the curve predicted by the theory of an isolated droplet.

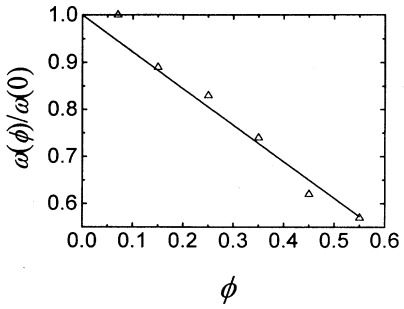

FIG. 7. The characteristic relaxation rate $\omega(\phi)$, reduced by its theoretical value $\omega(0)$, as a function of volume fraction ϕ. The data extrapolate to 1.0 as ϕ approaches zero, indicating the agreement of the measurements with the theory in the limit of isolated droplets. The smooth curve is an empirical linear fit.

which we obtain; however, this theory was restricted to the case of equal viscosities of the oil and water. In our experimental system, the droplet viscosity is an order of magnitude higher than the viscosity of the solvent. Since under these conditions the relaxation rate of the shape fluctuations of an isolated droplet is less sensitive to the viscosity of the solvent, it is plausible that the effects of the solvent-mediated interactions considered by the theory are less effective as well.

The ϕ dependence of the amplitude of the fluctuations exhibits different behavior. We show this in Fig. 8, where we plot the shape correlation function amplitude $R^2\Delta\sigma(t=0;\phi)/\sigma_0$, normalized by the theoretical value at $\phi=0,52$ Å^2. We designate the normalized amplitude more compactly by $\Delta\sigma(\phi)/\Delta\sigma(0)$. The data increase sharply, by a factor of about 2 at higher volume fractions. This increase in the amplitude of the shape fluctuations with ϕ is very surprising. It suggests that the energy driving shape fluctuations increases as ϕ increases. A possible source for this extra energy is the energy of translational motion, which may couple to shape fluctuations through collisions of the droplets. According to this view, we attribute the strong nonlinear increase of the amplitude of shape fluctuations to the rapid increase of the frequency of collisions as the system becomes denser. The probability of two droplets colliding should

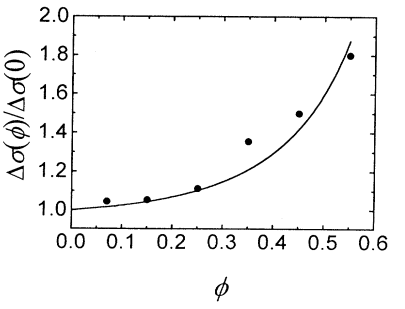

FIG. 8. The amplitude of the shape fluctuation correlation function, reduced by its theoretical value, as a function of volume fraction ϕ. The smooth curve is a fit to a simple model that attributes the amplitude dependence to collisions.

scale with the number of pairs of droplets touching one another, which is given by $\phi g(2,\phi)$, where $g(2,\phi)$ is the pair correlation function evaluated at the contact distance $2R$. This suggests a functional form for the normalized shape fluctuation amplitude $\Delta\sigma(\phi)/\Delta\sigma(0) = 1 + C\phi g(2,\phi)$. The expression assigns extra deformation to those droplets that are in contact with one or more neighbors; the fraction these colliding drops make out of the total number of drops is proportional to $\phi g(2,\phi)$. We treat C as adjustable and use the Carnahan-Starling equation of state for hard spheres, $g(2,\phi)=(1-\phi/2)/(1-\phi)^3$ [28]. The fit with $C=0.2$ is shown in Fig. 8 as the smooth curve. We obtain good agreement with the measured shape fluctuation amplitudes. We emphasize, however, that while this model gives reasonable agreement with data, it is nevertheless only a crude approximation. In particular, very recent work by Cai suggests that our expression is fundamentally wrong at low volume fraction [29]. Thus, whereas our expression gives C as the coefficient for the linear term in an expansion of $\Delta\sigma(\phi)/\Delta\sigma(0)$ in powers of ϕ, Cai's analytic calculation of this first coefficient gives $3k_BT/2\pi\Gamma R^2 \approx 4\times10^{-7}$. At higher ϕ, however, our data and our model expression do agree qualitatively with Cai's two-dimensional simulation of droplet shape fluctuations. Another possibility is that the shapes of neighboring droplets may fluctuate in a correlated way at higher ϕ. In that case, the measured $\Delta\sigma(\phi)/\Delta\sigma(0)$ may reflect the effects of spatially correlated amplitude fluctuations whose existence was ignored in deriving Eq. (22). Alternatively, it is also possible that the translational motion of the liquid droplets differs in some way from that of hard spheres, contrary to what we assumed in isolating the contribution of the shape fluctuations. This could also have the effect of modifying the measured amplitude at higher ϕ.

All of the data discussed to this point involved emulsions whose volume fractions were well below the limit of random close packing, and thus possessed liquidlike translational dynamics. However, since droplets are deformable, we can prepare emulsions with much higher volume fractions; then their translational motion is arrested, much like a colloidal glass. Nevertheless, we continue to see in DWS measurements an early decay on a time scale that seems to evolve continuously from the time scale of the shape fluctuations of droplets in less concentrated emulsions. We illustrate this behavior in Fig. 9, where we plot the inverted correlation functions for a series of volume fractions of the emulsion made from the oil with the lower viscosity of 12 cP. At low volume fractions, the shape fluctuations are clearly distinguished from the translational motion as an early-time region of lower slope on the logarithmic plots of the inverted correlation functions. Here, the translational motion persists after the shape fluctuations have decayed, reflecting the diffusive motion of the droplets. By contrast, as ϕ is increased, the translational motion is depressed at longer times; for $\phi=0.65$ and above, it is fully arrested, suggesting that all the remaining dynamics result solely from the shape fluctuations. We cannot give a full analysis of these measurements. A starting point

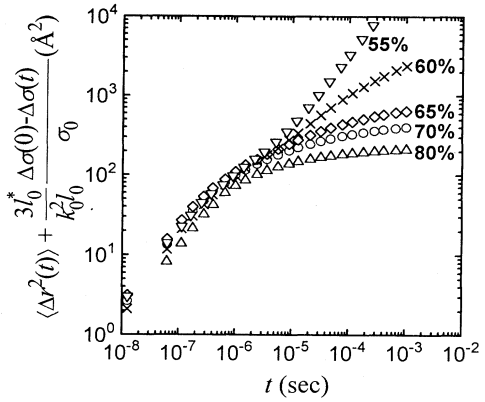

FIG. 9. Inverted DWS correlation functions from a series of dense and compressed emulsions of low viscosity oil. At $\phi=0.55$, translational motions are still evident as an increase of the slope of the correlation function on a logarithmic plot. Translations are arrested in highly compressed emulsions and the increase does not occur. The early-time behavior of the correlation functions is similar, however, which suggests that shape fluctuations are present in highly compressed emulsions.

for understanding compressed emulsions, however, is furnished by the example of the colloidal glass of rigid spheres [30]. At and above the glass transition, this system becomes nonergodic, so that the decay of the properly averaged autocorrelation function saturates at a finite value [31]. The cause of this saturation is the arrest of translational motions: particles do not execute displacements past some maximum value. Therefore, in compressed emulsions, shape fluctuations can remain significant in comparison with translations for longer times. In fact, when the translational motion is completely arrested at high ϕ, even the more slowly relaxing shape fluctuations of droplets of high viscosity oils can be resolved. Thus, we can obtain some idea of the separate contributions of shape fluctuations and translations to the dynamics of compressed emulsions by studying the effect of the oil viscosity. Shown in Fig. 10 are the measured

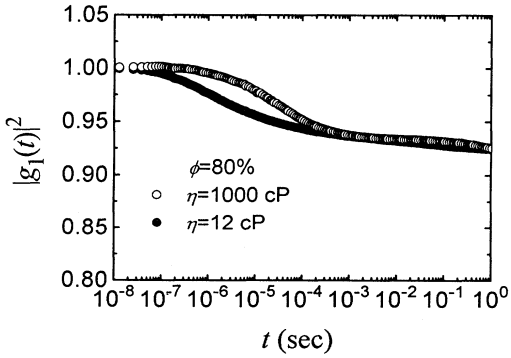

FIG. 10. The square of the field correlation function obtained from highly compressed emulsions of low and high viscosity oils. The correlation functions decay to a plateau that is independent of viscosity, while the time scale of the decay increases with viscosity.

intensity autocorrelation functions obtained from two emulsions with $\phi=80\%$. The solid symbols are the data for an emulsion of 12 cP oil, while the open symbols are for one of 1000 cP oil. Both sets of data exhibit a decay to the same absolute level, but the characteristic times are markedly different. Although only the initial decay is shown in Fig. 10, at longer times both sets of data decay fully, presumably due to slow relaxations of droplet configurations. Thus the measured correlation functions are automatically obtained with the proper ergodic averaging [31]. The inverted data are shown in Fig. 11, where the solid and open symbols again represent the data for the 12 and 1000 cP oils, respectively. The two sets of data saturate at the same final value, but the characteristic relaxation time for the emulsion of the less viscous oil is somewhat more than one order of magnitude shorter than that of the emulsion of the more viscous oil. The ratio of the two relaxation times is substantially less than the ratio of the viscosities, however, that would be expected from the viscosity dependence of the characteristic relaxation times of isolated droplets. The observed deviation from the expected behavior indicates that the shape fluctuation relaxation rate in a highly compressed emulsion is not controlled solely by the viscosity of the oil, and, instead, additional effects also contribute.

Finally, the fact that the saturation value of the decay of the correlation function is completely independent of viscosity indicates that it does not depend on the dynamics. Instead, it presumably relates to the effects of elasticity of these concentrated emulsions; the elastic modulus is in fact found to be independent of the viscosity of the oil [32]. Moreover, the ϕ dependence of the saturation level tracks that of elastic modulus [32]. This demonstrates the intrinsic relationship between the shape fluctuations of the droplets and the macroscopic properties of the emulsion.

VI. CONCLUSIONS

In this paper we have generalized the theory of diffusing-wave spectroscopy by incorporating the effects of amplitude fluctuations in the scattering intensity. The

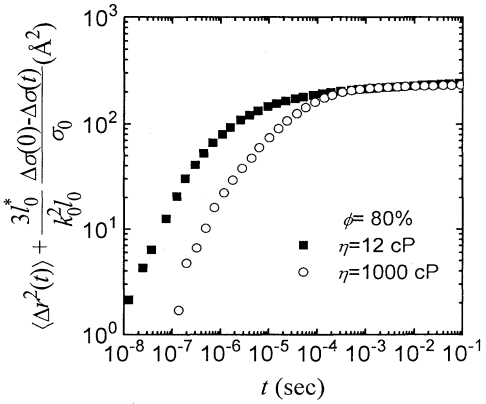

FIG. 11. The data of Fig. 10 in inverted form.

formulas we derived can be applied to study dynamic phenomena in which the form factor is time dependent, and the amplitude fluctuations of the scattered light reflect the dynamics of the shape, size, or rotation of scatterers. The detection of these fluctuations makes DWS a more generally useful and applicable technique. We apply this method to the study of thermally induced shape fluctuations of emulsion droplets whose geometry is controlled by surface tension. Since the surface potential energy of a droplet is much higher than $k_B T$, the deformation of a drop induced by the thermal energy is only a small fraction of its size. This deformation would not be detectable using conventional dynamic light scattering because of its small amplitude and fast relaxation. However, it is feasible using DWS, since the decay of the correlation function results from the combined fluctuations of the large number of scatterers that comprise the scattering path, allowing minute changes in each individual scatterer to be detected. Here, we are able to probe changes in the shapes of the scatterers corresponding to length scales as short as a few angstroms.

From our generalization of the theory for DWS we isolate the contribution of the shape fluctuations and investigate the ϕ dependence of the characteristic relaxation rate and amplitude of the fluctuations. Very good agreement is obtained between the theory of an isolated droplet and experimental values at low volume fractions. The relaxation behavior exhibits a distinctly nonexponential decay. We conclude that in addition to the lowest mode ($l=2$) higher order fluctuating modes are excited and relax with shorter time constants. However, we found a remarkable scaling behavior of the relaxation process over volume fraction. All data can be scaled onto the correlation function predicted for the shape relaxation of an isolated droplet. Upon extrapolating the scaling functions to $\phi=0$, excellent agreement with the theoretically predicted amplitude and characteristic relaxation rate is observed. The characteristic relaxation rate exhibits a linear decrease with volume fraction, while the amplitude of the shape fluctuations shows a nonlinear increase. We speculate that the ϕ dependence of the amplitude of the shape fluctuations is a consequence of collisions and the additional energy transferred from interparticle interaction into the interfacial degrees of freedom. We account for these collisions by relating the ϕ-dependent shape fluctuation amplitude to the radial distribution function at contact. The rapid increase of collisions with volume fraction results in a strong, nonlinear increase in the amplitude of shape fluctuations. However, to fully account for the ϕ dependence, further theoretical work is clearly required; for example, recent computer simulations also exhibit similar behavior [29].

The flexibility of liquid droplets is one of their most distinguishing features; it controls many of their unique properties. The shape fluctuations studied here directly probe this flexibility. Moreover, as the volume fraction increases, shape fluctuations can lead to significant modifications of the properties of the interacting droplets. In particular, these shape fluctuations may make a significant contribution to the onset of an elastic modulus, which occurs as ϕ is increased sufficiently to deform the droplets permanently. The effects of increasing interactions on the shape fluctuations may provide new insight into this important problem. Another important issue is the potential connection between coalescence and shape fluctuations of emulsion droplets. In order to induce coalescence, rupture of the liquid film between the droplets must take place. The rupture of the thin film is usually due to thermal or mechanical fluctuations which result in the stretching of the liquid surface and the formation of surface waves that grow in amplitude until coalescence occurs. Thus the techniques reported here may provide a method for probing the stability of emulsions; shape fluctuations may be a critical precursor of coalescence, one of the key mechanisms by which an emulsion is destroyed.

ACKNOWLEDGMENTS

We acknowledge valuable discussions with J. Bibette, W. Cai, T. Lubensky, and S. T. Milner.

[1] P. Becher, *Emulsion: Theory and Practice* (Reinhold, New York, 1965).
[2] L. L. Schramm, *Emulsions: Fundamentals and Applications in the Petroleum Industry* (American Chemical Society, Washington, DC 1992).
[3] R. H. Katyl and U. Ingard, Phys. Rev. Lett. **20**, 248 (1968).
[4] M. K. Sanyal, S. K. Sinha, K. G. Huang, and B. M. Ocko, Phys. Rev. Lett. **66**, 628 (1991).
[5] J. S. Huang, S. T. Milner, B. Farago, and D. Richter, Phys. Rev. Lett. **59**, 2600 (1987).
[6] B. Farago, D. Richter, J. S. Huang, S. A. Safran, and S. T. Milner, Phys. Rev. Lett. **65**, 3348 (1990).
[7] C. R. Safinya, D. Roux, G. S. Smith, S. K. Sinha, P. Dimon, N. A. Clark, and A. M. Belloq, Phys. Rev. Lett. **57**, 2718 (1986).
[8] H. P. Duwe, J. Kaes, and E. Sackmann, J. Phys. (Paris) **51**, 945 (1990).
[9] D. J. Pine, D. A. Weitz, P. M. Chaikin, and E. Herbolzheimer, Phys. Rev. Lett. **60**, 1134 (1988).
[10] D. A. Weitz and D. J. Pine, in *Dynamic Light Scattering*, edited by W. Brown (Oxford University Press, Oxford, 1992).
[11] D. A. Weitz, J. X. Zhu, D. J. Durian, H. Gang, and D. J. Pine, Phys. Scr. **T49**, 610 (1993).
[12] J.-Z. Xue, X.-L. Wu, D. J. Pine, and P. M. Chaikin, Phys. Rev. A **45**, 989 (1992).
[13] J. X. Zhu, D. A. Weitz, and R. Klein, in *Photonic Band Gaps and Localization,* edited by C. Soukoulis (Plenum, New York, 1993).
[14] A. J. C. Ladd, H. Gang, J. X. Zhu, and D. A. Weitz, Phys. Rev. Lett. **74**, 318 (1995).
[15] A. J. C. Ladd, H. Gang, J. X. Zhu, and D. A. Weitz, Phys. Rev. E (to be published).

[16] P. E. Wolf, G. Maret, E. Akkermans, and R. Maynard, J. Phys. (Paris) **49**, 63 (1988).
[17] S. T. Milner and S. A. Safran, Phys. Rev. A **36**, 4371 (1987).
[18] H. Lamb, *Hydrodynamics* (Dover, New York, 1932).
[19] R. G. Cox, J. Fluid Mech. **37**, 601 (1969).
[20] S. J. Choi and W. R. Schowalter, Phys. Fluids **18**, 420 (1974).
[21] M. Kerker, *The Scattering of Light and Other Electromagnetic Radiation* (Academic, New York, 1969).
[22] J. Bibette, J. Colloid Interface Sci. **147**, 474 (1991).
[23] P. N. Pusey and W. van Megen, Nature **320**, 340 (1986).
[24] J. Ricka, Appl. Opt. **32**, 2860 (1993).
[25] W. Hess and R. Klein, Adv. Phys. **32**, 173 (1983).
[26] E. J. Hinch, J. Fluid Mech. **72**, 499 (1975).
[27] M. Schwartz and S. F. Edwards, Physica A **167**, 589 (1990).
[28] J. F. Brady, J. Chem. Phys. **99**, 567 (1993).
[29] W. Cai (unpublished).
[30] W. van Megen and S. M. Underwood, Phys. Rev. E **49**, 4206 (1994).
[31] P. N. Pusey and W. van Megen, Physica A **157**, 705 (1989).
[32] T. G. Mason, J. Bibette, and D. A. Weitz, Phys. Rev. Lett. **75**, 2051 (1995).